

See discussions, stats, and author profiles for this publication at: <https://www.researchgate.net/publication/273064990>

A Novel Alkaline Hemicellulosic Heteroxylan Isolated from Alfalfa (Medicago sativa L.) Stem and Its Thermal and Anti-inflammatory Properties

ARTICLE in JOURNAL OF AGRICULTURAL AND FOOD CHEMISTRY · MARCH 2015

Impact Factor: 2.91 · DOI: 10.1021/acs.jafc.5b00063 · Source: PubMed

CITATION

1

READS

74

6 AUTHORS, INCLUDING:



Lei Chen

Chinese Academy of Sciences

17 PUBLICATIONS 71 CITATIONS

[SEE PROFILE](#)



Bona Dai

Shanghai Jiao Tong University

8 PUBLICATIONS 26 CITATIONS

[SEE PROFILE](#)



Liangli Lucy Yu

University of Maryland, College Park

155 PUBLICATIONS 5,083 CITATIONS

[SEE PROFILE](#)

A Novel Alkaline Hemicellulosic Heteroxylan Isolated from Alfalfa (*Medicago sativa* L.) Stem and Its Thermal and Anti-inflammatory Properties

Lei Chen,[†] Jie Liu,[†] Yaqiong Zhang,[†] Yuge Niu,[†] Bona Dai,[‡] and Liangli (Lucy) Yu^{*,†,§}

[†]Institute of Food and Nutraceutical Science, School of Agriculture and Biology, and [‡]Instrumental Analysis Center, Shanghai Jiao Tong University, Shanghai 200240, China

[§]Department of Nutrition and Food Science, University of Maryland, College Park, Maryland 20742, United States

S Supporting Information

ABSTRACT: A novel hemicellulosic polysaccharide (ACAP) was purified from the cold alkali extraction of alfalfa stems and characterized as a heteroxylan with a weight-average molecular weight of 7.94×10^3 kDa and a radius of 58 nm. Structural analysis indicated that ACAP consisted of a 1,4-linked β -D-Xylp backbone with 4-O-MeGlcA and T-L-Araf substitutions at O-2 and O-3 positions, respectively. Transmission electron microscopy (TEM) examination revealed the entangled chain morphology of ACAP molecules. The evaluation of thermal degradation property revealed a primary decomposition temperature range of 238.8–314.0 °C with an apparent activation energy (E_a) and a pre-exponential factor (A) of 220.0 kJ/mol and 2.81×10^{24} /s, respectively. ACAP also showed significant inhibitory activities on IL-1 β , IL-6, and COX-2 gene expressions in cultured RAW 264.7 mouse macrophage cells. These results suggested the potential utilization of ACAP in functional foods and dietary supplement products.

KEYWORDS: alfalfa polysaccharide, hemicellulosic heteroxylan, structural analysis, thermal decomposition, anti-inflammatory effect

INTRODUCTION

Alfalfa (*Medicago sativa* L.) is the second most widely cultivated leguminous crop around the world. The worldwide production of alfalfa was about 436 million tons in 2006, and the production area reached approximately 30 million hectares in 2009.¹ Alfalfa has mainly been cultivated as an important forage crop because of its abundant and excellent proteins in its leaves.² However, the value of alfalfa stem, a large proportion of the total accumulated biomass, has been ignored.

Alfalfa stems might contain large amount of polysaccharides, including hemicelluloses and a group of pectic substances.^{3–5} For instance, polysavone, a crude hot water extract of alfalfa, contained approximately 18% of polysaccharides and was able to improve the antioxidant status and immunity of broiler chickens.^{6,7} Additionally, water-extractable crude polysaccharides from alfalfa showed antioxidant^{8,9} and lipid-lowering¹⁰ effects using the evaluation model of rabbit and laying hen, respectively. Recently, a study has purified four alfalfa polysaccharides from the crude polysaccharides extracted with the enzyme method and then studied protective effects on hepatocytes in vitro.¹¹ However, little information has been available for the chemical structures of alfalfa polysaccharides, although monosaccharide composition was investigated for the four alfalfa polysaccharides.

Hemicellulosic polysaccharides and their derivatives have been recognized for their potential health benefits including modulation of colon microflora and stimulation of lymphocytes.^{12,13} Moreover, hemicellulose has been widely applied in the food industry as thickeners, stabilizers, emulsifiers, and so on.¹⁴ Alfalfa stems are rich in hemicellulosic polysaccharides.^{3,5} To date, the hemicellulosic polysaccharide with a clear chemical

structure has not been reported from alfalfa stem, and little has been known about their potential anti-inflammatory activity, although alfalfa crude polysaccharide extracts have been studied for their potential antioxidant and lipid-lowering activities, as well as protection of hepatocytes.^{8–11}

In the present work, a novel heteroxylan (ACAP) was purified from the alkali extract of alfalfa stem, and its chemical and molecular structures were characterized. Moreover, the thermal stability and pyrolysis pattern of ACAP were determined, along with its potential anti-inflammatory activity. To our knowledge, this is the first study in which thermal degradation analysis and in vitro anti-inflammatory determination have been performed on a purified hemicellulosic polysaccharide from alfalfa stem. The results from this research could be used to develop value-added utilization of alfalfa and benefit local agricultural economies.

MATERIALS AND METHODS

Materials. The alfalfa sample was obtained from the Gansu province of China and dried at room temperature. The alfalfa stem was separated and pulverized into powder (200 mesh) using an IKA mill (IKA, A11, Germany). TRIzol reagent was purchased from Invitrogen (Carlsbad, CA, USA). An iScript Advanced cDNA Synthesis kit was purchased from Bio-Rad (Hercules, CA, USA). RAW 264.7 mouse macrophage cells were obtained from the Chinese Academy of Sciences (Shanghai, China). Lipopolysaccharide (LPS) from *Escherichia coli* O111:B4 was obtained from Millipore (Bedford, MA, USA). Other reagents for

Received: January 5, 2015

Revised: February 25, 2015

Accepted: March 2, 2015

Published: March 2, 2015

isolation and analysis were of analytical grade and used without further purification.

Fractionation and Purification of Hemicellulosic Polysaccharides. The ground powders were suspended in a 95% ethanol solution and heated to 75 °C for 2 h to remove small molecular components. After centrifugation at 4500g for 10 min at 4 °C, the obtained residues were suspended in a 15-fold volume of distilled water (DD H₂O, w/v) and kept at 80 °C for 2 h to remove the water-soluble polysaccharides and proteins. Each step was repeated three times. The water-insoluble residue was extracted four times by a 20-fold volume of 1 M NaOH at ambient temperature with continuous stirring for 12 h. The alkali extract was neutralized with HCl solution and precipitated with a 4-fold volume of 95% ethanol (v/v) and washed three times with 75% ethanol, followed by lyophilization to obtain the crude hemicellulosic polysaccharides of alfalfa stem.

The crude polysaccharides were subjected to further fractionation by membrane ultrafiltration (Minimate TFF system, Pall Corp., Port Washington, NY, USA) with a molecular weight (MW) cutoff of 10 kDa to obtain the cold alkali-extractable polysaccharide molecules of alfalfa stem (ACAP) with MW larger than 10 kDa. ACAP was further purified by gel filtration on a Sephadryl S-400 Superfine column (80 × 1.6 cm i.d., Amersham Pharmacia Biotech, Uppsala, Sweden) eluted with DD H₂O at 1.0 mL/min. The collected fraction was freeze-dried prior to further analyses.

Molecular Weight and Size. A particle size analyzer (Zetasizer Nano-ZS90, Malvern Instruments Ltd., Malvern, Worcs, UK) was used to determine the molecular weight and size of ACAP. In brief, the purified ACAP was dissolved in DD H₂O and heated at 80 °C for 2 h to avoid aggregation. The dispersed solution was diluted to 1.00, 0.75, 0.50, 0.25, and 0.10 mg/mL. The laser light scattering was measured for these samples using a static light scattering (SLS) to obtain the Debye plot, which was used to calculate the weight-averaged molecular weight (M_w) according to the Rayleigh equation (eq 1).¹⁵ To avoid the interactions of molecules, 0.05 mol/L NaOH solution was prepared to dissolve ACAP molecules for size determination using the SLS method. The molecular size was obtained at the concentration of 0.25 mg/mL.

$$\frac{KC}{R_\theta} = \left(\frac{1}{M_w} + 2A_2 C \right) \times P(\theta) \quad (1)$$

In the equation, K , M_w , A_2 , and C represent optical constant, sample molecular weight, second virial coefficient, and sample concentration, respectively. The Rayleigh ratio (R_θ) indicates the ratio of scattered light to incident light of the sample, whereas $P(\theta)$ means the angular dependence of the sample scattering intensity. $P(\theta)$ reduces to 1 when the particles are much smaller than the wavelength of incident light. The M_w (Da or g/mol) was then determined from the intercept at zero concentration ($C \rightarrow 0$) according to $KC/R_\theta = 1/M_w$.

Chemical Composition Analysis. The total carbohydrate and uronic acid contents were determined using the phenol–sulfuric acid¹⁶ and *m*-hydroxydiphenylsulfuric acid methods,¹⁷ respectively. The protein content was analyzed by bicinchoninic acid protein assay (BCA) as described previously.¹⁸

The compositions of neutral sugars and uronic acids of ACAP were determined by PMP-HPLC method.¹⁹ ACAP (10 mg) was hydrolyzed with 200 μL of 4 M trifluoroacetic acid (TFA) at 110 °C for 2 h. TFA in the reaction mixture was removed under nitrogen stream with the addition of 200 μL of methanol and repeated three times. The hydrolysates were dissolved in 50 μL of 0.3 M NaOH solution and reacted at 70 °C for 100 min with the addition of 50 μL of 0.5 M 1-phenyl-3-methyl-5-pyrazolone (PMP) solution in methanol. After cooling to room temperature, the mixture was neutralized with 0.3 M HCl, followed by the addition of DD H₂O to the final volume of 1 mL. An equal volume of dichloromethane was added, vortex-mixed, and repeated three times to remove the residual PMP. The sugar standard was prepared by mixing a solution of L-rhamnose (Rha), L-fucose (Fuc), L-arabinose (Ara), D-xylose (Xyl), D-mannose (Man), D-galactose (Gal), D-glucose (Glc), D-glucuronic acid (GlcP), and D-galactouronic acid (GalP). The mixed standard also went through the above procedures except for hydrolysis with TFA. The obtained upper layer solution

was filtered through a 0.45 μm Millipore filter and subjected to HPLC analysis at 250 nm with an Inertsil ODS-3 column (100 mm × 2.1 mm i.d., 2 μm, GL Sciences Inc., Tokyo, Japan). The chromatographic separation was carried out at 30 °C under the elution conditions of 0.1 M phosphate buffer (pH 6.7)/acetonitrile at a ratio of 80:20 (v/v).

Linkage Analysis by Methylation. For the existence of uronic acid, ACAP was first reduced using NaBD₄²⁰ and then methylated using methyl iodide (CH₃I) in a NaOH–DMSO dry slurry as reported previously,²¹ followed by hydrolysis with 4 M TFA for 2 h at 121 °C. Samples were reduced with 0.1 mL of 10 mg/mL NaBD₄ and then acetylated by 100 μL of acetic anhydride. Afterward, the obtained partially methylated alditol acetate (PMAA) mixtures were examined using an Agilent 7890A-5975C GC-MS system (Agilent Technology, Santa Clara, CA, USA) equipped with a HP-5 capillary column (30 m × 0.32 mm i.d., 0.25 μm film). The GC conditions were as follows: initial temperature, 50 °C, increased at 30 °C/min to 150 °C, increased at 3 °C/min to 220 °C, and finally increased to 300 °C at 30 °C/min and held for 10 min; injector temperature, 250 °C; interface temperature, 280 °C. The MS conditions were as follows: ion source temperature, 300 °C; ionization energy, 70 eV; detector voltage, 1.5 kV; mass range, 50–550. Glycosidic linkages of ACAP were determined by comparing the GC-MS results of the PMAs with mass spectrum patterns from the online database.²² The molar ratios of individual linkage residues were calculated on the basis of the peak areas and response factors for individual sugars in the TIC as described previously.²³

Spectroscopic Analysis. The Fourier transform infrared (FT-IR) spectrum of ACAP was recorded using a FT-IR spectrometer (Nicolet 6700, Thermo Fisher, USA) in the range of 4000–400 cm⁻¹ using the KBr disk method.

One- and two-dimensional measurements (including ¹H NMR, ¹³C NMR, DEPT 135, HH COSY, TOCSY, and HSQC) of ACAP were recorded on a 600 MHz NMR spectrometer (Bruker Avance III HD) with a 5 mm TCI CryoProbe (¹³C/¹H/¹⁵N) at 25 °C using D₂O as the solvent at a final concentration of 40 mg/mL.

Microscopic Analysis. To observe the microstructure of ACAP, sodium dodecyl sulfate (SDS) was selected as a surfactant to disperse the polysaccharide in aqueous solution as described previously.^{24,25} ACAP aqueous solution was prepared at a concentration of 1 mg/mL, followed by the addition of an equal volume of SDS solution (1 mg/mL). The mixture was then heated at 80 °C for 2 h with constant stirring and diluted with DD H₂O to a final concentration of 5 μg/mL. A droplet of ACAP solution was deposited on the carbon film specimen (200 mesh, Beijing Zhongjingkeyi Technology, Beijing, China). Transmission electron microscopy (TEM, Tecnai G2 Spirit BIOTWIN, FEI, USA) with an accelerating voltage of 120 kV was applied to visualize the molecular morphology of the ACAP samples after they were dried at ambient temperature and humidity.

Isoconversional Thermal Characteristics. A simultaneous thermal analyzer (SDT-Q600, TA Instruments, USA) was used to determine the thermodynamic characteristics of the ACAP. ACAP samples (5 mg for each) were treated at three different heating rates (including 5, 10, and 20 °C/min from 50 to 600 °C) under a nitrogen atmosphere at a flow rate of 100 cm³/min. The obtained data were then analyzed by the isoconversional Flynn–Wall–Ozawa (FWO) method (eq 2) as previous studies reported.^{26,27}

$$\log \beta = \log \frac{AE_a}{Rg(\alpha)} - 2.315 - 0.4567 \frac{E_a}{RT} \quad (2)$$

$g(\alpha) = \int_0^\alpha da/f(\alpha)$; β is the heating rate; R is the general gas constant; A stands for the pre-exponential factor; E_a is the apparent activation energy; and T is the temperature at the conversion α . This model-free approach was applied to obtain a plot of $\log \beta$ versus $1/T$ at different conversion rates for calculation of $-E_a/R$ as the slope.

Following the calculation of an average E_a value, lnA was obtained by the compensation effect relationship as eq 3. The compensation parameters of a and b could be obtained from a plot of lnA versus E_a from a model-fitting approach using Coats–Redfern eq 4 with T' being the average experimental temperature. In addition, the experimental lnA could be calculated according to eq 3.

$$\ln A = aE_a + b \quad (3)$$

$$\ln \frac{g(\alpha)}{T^2} = \ln \left[\left(\frac{\alpha R}{\beta E_a} \right) \left(1 - \frac{2RT'}{E_a} \right) \right] - \frac{E_a}{RT} \quad (4)$$

The thermal analysis data were analyzed using Universal Analysis 2000 software (version 4.5A, TA Instruments, USA) and MS Excel 2013.

Anti-inflammatory Activity Determination. To analyze the anti-inflammatory effect of ACAP, RAW 264.7 mouse macrophage cells were selected to detect the inhibition of IL-1 β , IL-6, and COX-2 gene expressions. The aqueous ACAP solution was prepared at two treatment concentrations of 10 and 50 μ g/mL. RAW 264.7 cells were cultured in 6-well plates for 24 h to reach an 80% confluence before the addition of ACAP-containing media. After further incubation for 24 h, LPS was pipetted into the medium at a final concentration of 10 ng/mL and incubated for another 4 h at 37 °C under 5% CO₂. The macrophage cells were collected and washed for RNA isolation and real-time PCR analysis according to previously described laboratory procedures.^{28,29} In general, total RNA was isolated using the TRIzol reagent, followed by the reverse transcription cDNA using a iScript Advanced cDNA Synthesis kit. Real-time PCR was carried out on an ABI 7900HT Fast Real-Time PCR System (Applied Biosystems, Foster City, CA, USA) using the following PCR conditions: 50 °C for 2 min, 95 °C for 10 min, and 46 cycles of amplification at 95 °C for 15 s and 60 °C for 1 min.

Statistical Analysis. Significant differences between means were evaluated by one-way ANOVA followed by Tukey's multiple-comparison test to identify differences in means using SPSS for Windows (version rel. 18.0, SPSS Inc., Chicago, IL, USA). Statistical significance was declared at $P < 0.05$.

RESULTS AND DISCUSSION

Preparation of ACAP. After successive extractions with 95% ethanol and hot water, the crude cold alkali-soluble fraction was obtained, and the yield was found to be 8.47% on a per alfalfa stem dry weight basis. The composition analysis indicated that ACAP was composed of approximately 95.42% (w/w) of total carbohydrate, which contained about 9.38% uronic acid, whereas no protein was detected in the crude ACAP.

After sequential purification by ultrafiltration and gel permeation chromatography, a single fraction was obtained and designated ACAP (Figure S1 in the Supporting Information). The PMP-HPLC analysis showed that ACAP was composed of xylose, glucuronic acid, and arabinose in a molar ratio of 23:3:1. The M_w of ACAP was calculated to be 7.94 $\times 10^3$ kDa (or 7.94 $\times 10^6$ g/mol), whereas A_2 was calculated to be 2.45 $\times 10^{-4}$ from the gradient of the Debye plot (Figure S2 in the Supporting Information). The value of A_2 (>0) indicated that the aqueous solution of ACAP was a stable system. The radius of gyration (R_g) was determined to be 58 \pm 6 nm for ACAP. The SLS method was applied to determine the molecular weight of ACAP because the commonly used size exclusion chromatographic analysis is not suitable for weight determination of branched polysaccharides.

Glycosidic Linkages of ACAP. ACAP was composed of a terminal arabinose (T-L-Araf), 1,3,4-D-xylose (Xylp), 1,2,4-D-Xylp, 1,4-D-Xylp, and a terminal glucuronic acid (T-D-GlcP α) in a molar ratio of 1:1.1:3.2:20.6:3.1, according to the PMAA analysis (Table 1). The ratio between terminal units (T-L-Araf and T-D-GlcP α) and the branching points (1,3,4-D-Xylp and 1,2,4-D-Xylp) was 0.95, indicating that the number of terminal units was approximately equal to the number of branching points in ACAP. These results indicated that ACAP might contain a \rightarrow 1)-D-Xylp-(4 \rightarrow backbone with T-L-Araf and T-D-GlcP α residues at the O-2 or O-3 site to form the side chains. Additionally, the

Table 1. Molar Ratio of Glycosidic Linkages in ACAP by Methylation Analysis

retention time (min)	PMAA ^a	mass fragments (<i>m/z</i>)	linkage type	molar ratio
10.632	1,4-O-Ac2-2,3,5-O-Me3-D-arabinitol	87, 101, 117, 129, 161	T-L-Araf	1.0
13.015	1,4,5-O-Ac3-2,3-O-Me2-D-xylitol	87, 101, 117, 129, 189	1,4-L-Xylp	20.6
13.314	1,2,4,5-O-Ac4-3-O-Me-D-xylitol	87, 129, 189	1,2,4-D-Xylp	3.2
13.637	1,3,4,5-O-Ac4-2-O-Me-D-xylitol	85, 99, 117, 127, 159, 201, 261	1,3,4-D-Xylp	1.1
22.046	1,5-O-Ac2-2,3,4,6-O-Me4-6-deutero-D-glucitol	87, 101, 117, 129, 146, 161, 206	T-D-GlcP α	3.1

^aAc, acetyl; Me, methyl.

degree of branching (DB) value of ACAP was calculated as 29% following the equation DB = (NT + NB) / (NT + NB + NL) as described by Hawker and others,³⁰ where NT, NB, and NL are the numbers of the terminal residues, branch residues, and linear residues, respectively.

FT-IR Spectrum. As shown in Figure S3 in the Supporting Information, most of the absorption bands could be assigned according to previous literature.^{31,32} The signals at 3431 and 2925 cm^{-1} originated from the stretching vibrations of OH and CH₂, respectively. The strong absorption at 1635 cm^{-1} was attributed to the H—O—H angle vibration of water, because hemicellulosic polymers usually reported to contain bound water. The absorptions at 1465, 1383, 1248, 1158, 1044, 989, and 897 cm^{-1} were the characteristic peaks of hemicelluloses. Among them, the two weak signals at 1158 cm^{-1} (the C—O—C vibration) and 989 cm^{-1} represented small amounts of arabinosyl side chains, which were only attached at positions of the xylopyranosyl backbone according to a previous study.³³ Moreover, the strong peak at 1044 cm^{-1} (the C—O, C—C stretching, or C—OH bending vibration) was a typical absorbance of xylopyranosyl units in hemicellulose, whereas the signal at 897 cm^{-1} was attributed to β -glycosidic linkages between monosaccharide units.^{34–36} In addition, the signal at 1420 cm^{-1} was from the symmetric stretching vibration of glucuronic acid groups in side chains.

Structural Characterization by NMR Analysis. The attributions of structural residues with different substitution patterns in the polysaccharide were determined by quantitative ¹H NMR (Figure 1A) and ¹³C NMR (Figure 1B) spectra, along with HSQC spectrum (Figure 1C) and single-bond (COSY) and multiple-bond (TOCSY) proton—proton correlations and HMBC spectra (Figure S4 in the Supporting Information). In the HSQC spectrum (Figure 1C), the anomeric region of ¹H is from 4.3 to 5.5 ppm, whereas the corresponding ¹³C is in the range of 90–110 ppm. The obtained assignments were confirmed according to the previous reports on hemicellulosic heteroxylan and summarized in Table 2. Consistent with the result of linkage analysis, β -1 \rightarrow 4-linked xylopyranosyl units were characterized to be dominant in ACAP by five primary peaks at 101.6 (4.38), 72.6 (3.17), 73.6 (3.45), 72.7 (3.68), and 62.9 (4.01 and 3.28) ppm, which were assigned to C1 (H1), C2 (H2), C3 (H3), C4 (H4), and C5 (H5) of the β -D-Xylp units, respectively. In addition, weak signals of α -4-O-MeGlcP α and T- α -L-Araf were identified to be in the side chains of β -D-Xylp backbone from the present spectra (Table 2). The results of linkage analysis, FT-IR

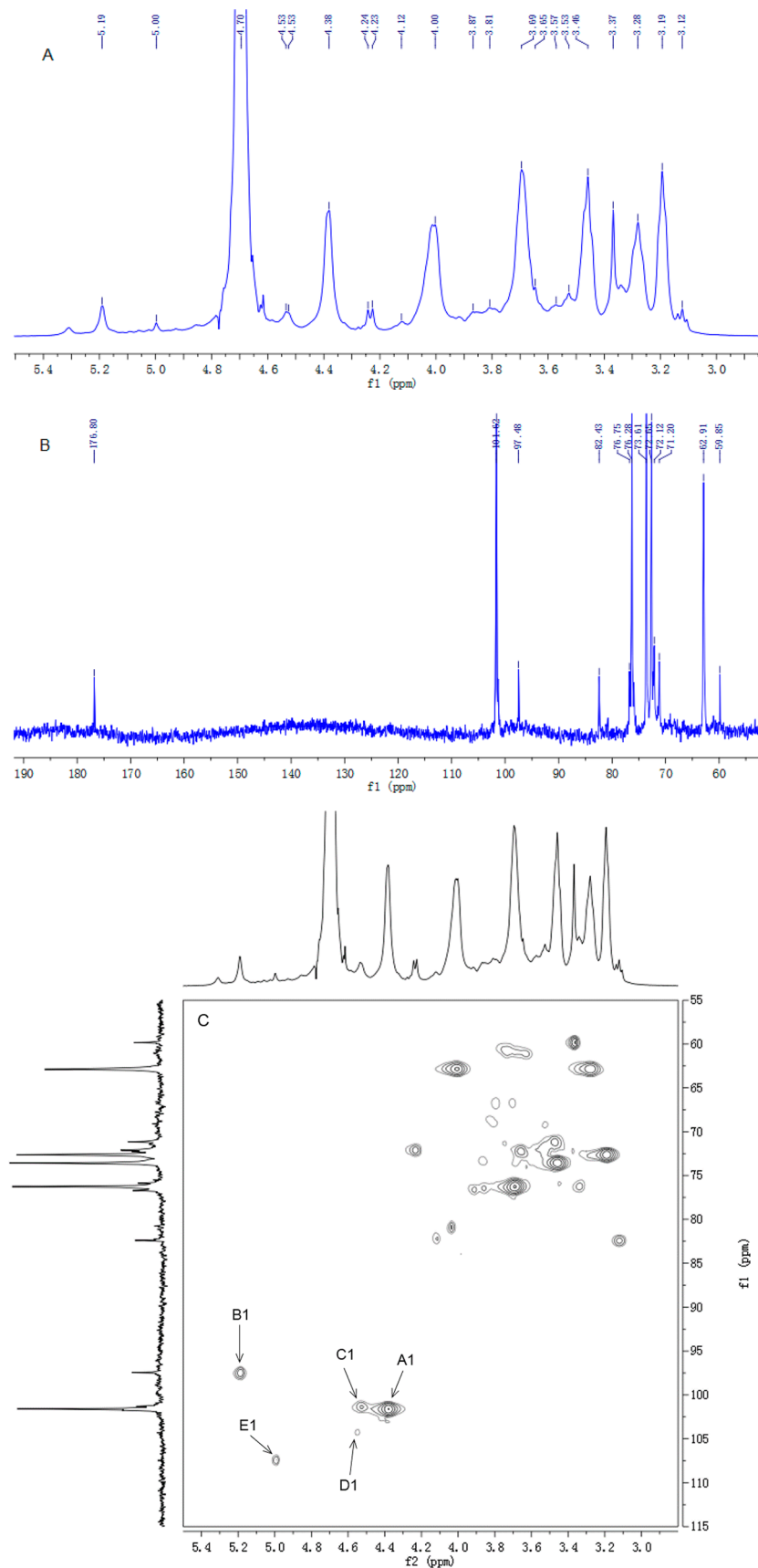


Figure 1. ^1H NMR (A), ^{13}C NMR (B), and HSQC (C) spectra (D_2O , 25°C) for ACAP. A1 means the correlation between C1 and H1 of residue A. Order of residues A, B, C, D, and E was consistent with Table 2.

Table 2. ^1H and ^{13}C NMR Chemical Shifts of ACAP Recorded in D_2O at 25 °C

no. ^a	residue	chemical shift, δ							
		1	2	3	4	5	OMe	COOH	
A	β -1,4-D-Xylp	H	4.38	3.18	3.45	3.68	4.01	3.28	
		C	101.62	72.64	73.57	76.28	62.85		
B	α -4-O-MeGlcA	H	5.19	3.48	3.18	3.12	4.23	3.38	
		C	97.49	71.21	71.54	82.42	72.11	59.83	176.88
C	β -1,2,4-D-Xylp	H	4.53	3.34	3.52	3.86	3.70		
		C	101.36	76.24	72.10	76.47	66.75		
D	β -1,3,4-D-Xylp	H	4.54	3.55	3.36	4.38			
		C	104.30	72.08	76.24	77.45			
E	T- α -L-Araf	H	4.99	4.03	3.99	4.12	3.63		
		C	107.43	80.90	83.91	82.22	61.09		

^aResidues A, B, C, D, and E were designated according to the decreasing order of proton peak intensity.

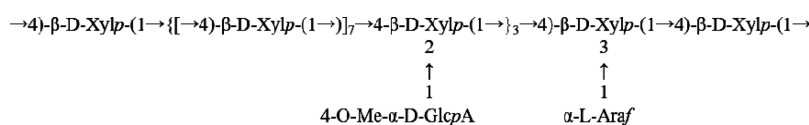


Figure 2. Proposed partial structure of the ACAP repeating unit.

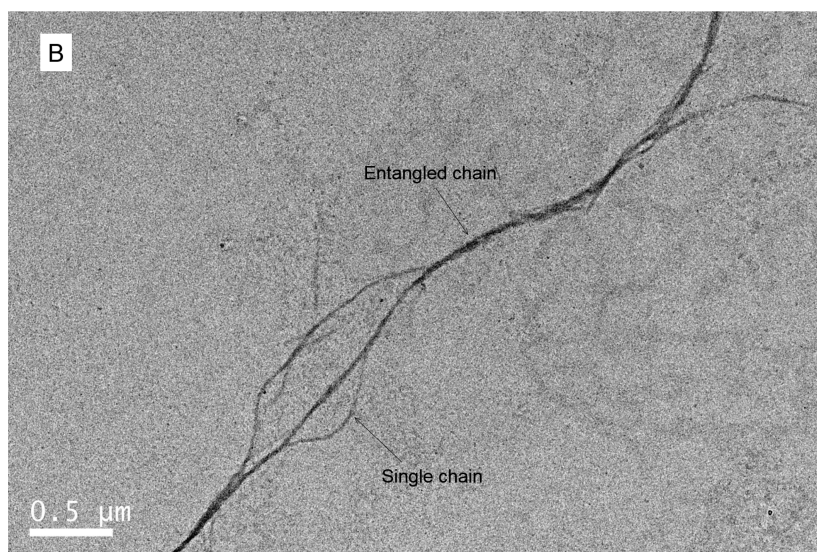
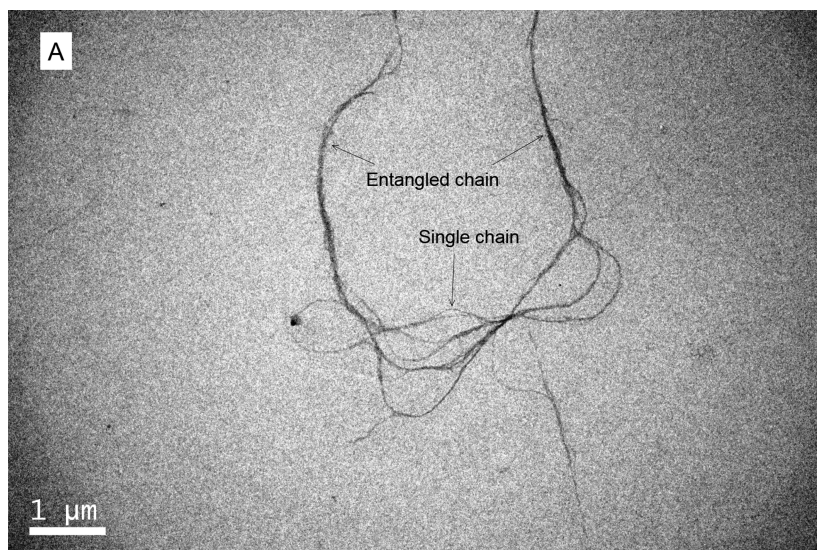


Figure 3. TEM images of ACAP in sodium dodecyl sulfate solution.

spectrum, and NMR analysis also indicated that ACAP contained no $-\text{OCH}_3$ group, which was different from other hemicellulosic heteroxylans. According to previous studies, hemicellulosic xylan often contains large amounts of $-\text{OCH}_3$ groups on the O-2 and/or O-3 sites of the xylan backbone. This difference might be explained by the fact that the alkali extraction procedure might result in the hydrolysis of potential $-\text{OCH}_3$ groups in ACAP. Additionally, the above result indicated that T-D-GlcA existed in the ACAP molecule as the form of α -4-O-MeGlcA. According to the present results and previous literature on the structure of hemicellulosic xylan,^{37–39} the primary structure of ACAP could be deduced as a β -1 \rightarrow 4-D-Xylp backbone with small amounts of α -4-O-MeGlcA and T- α -L-Araf in the side chains on the O-2 and O-3 sites, respectively (Figure 2).

Microscopic Morphology of ACAP. Morphological information is important to illustrate the fine structure of macromolecules intuitively. In the present study, TEM analysis was conducted to further observe the microstructure of ACAP. As shown in Figure 3, both single chain and entangled chain were observed in ACAP molecules under the experimental conditions. Similar to the triple-helical conformation of lentinan, ACAP molecules tended to form entangled chains, which contained even more than three single chains as shown in Figure 3A. Moreover, the approximately linear structure with minor branches from Figure 3B was consistent with the above results of methylation and NMR analysis.

Thermal Decomposition Analysis. The applicability of polysaccharide is also largely dependent on its thermal behavior. Thermal degradation characteristics of ACAP were determined from the curves of thermal gravity, differential thermal gravity, and second-time derivatives (TG, DTG, and D²TG) in the temperature range of 50–600 °C. As shown in Figure 4A, two steps of weight loss occurred in the thermogravimetric analysis. The major decomposition of polysaccharide structure occurred at 200–350 °C, because about 70% of the weight was lost within this temperature range. In addition, minor weight loss (~7%) occurred in the 50–150 °C range due to the loss of trapped water. Therefore, the weight at 150 °C was defined as 100% dry weight for the next degradation analysis of ACAP.

Three different heating rates were applied to identify the thermal degradation parameters of ACAP in the 150–600 °C range (Figure 4B) and deduced to a β value of 0 for each of the three temperatures (Figure 4C). The degradation characteristics are summarized in Table 3, where the parameters T_o , T_p , and T_s represent the onset, maximum, and shift decomposition temperatures, respectively, whereas WL_o, WL_p, and WL_s indicate the corresponding weight loss percentage parameters. As indicated in Table 3, the maximum degradation rate was observed at 278.6 °C (T_p) with a weight loss of 21.81% on a dry weight basis (WL_p), whereas ACAP experienced a rapid degradation in a narrow temperature range from the transition of T_p to T_s .

The apparent activation energy (E_a) and pre-exponential factor A were obtained by the isoconversional FWO method (Figure 5) at a conversion range from 0.3 to 0.7 with a 0.1 increment. The average E_a value was calculated as 220.0 kJ/mol, whereas the experimental $\ln A$ was obtained by the compensation effect relationship as eq 3 (Table S1 in the Supporting Information). The compensation parameters of a and b were obtained from a plot of $\ln A$ versus E_a (Figure S5 in the Supporting Information) using the Coats–Redfern equation (eq 4) (Table S2 in the Supporting Information).

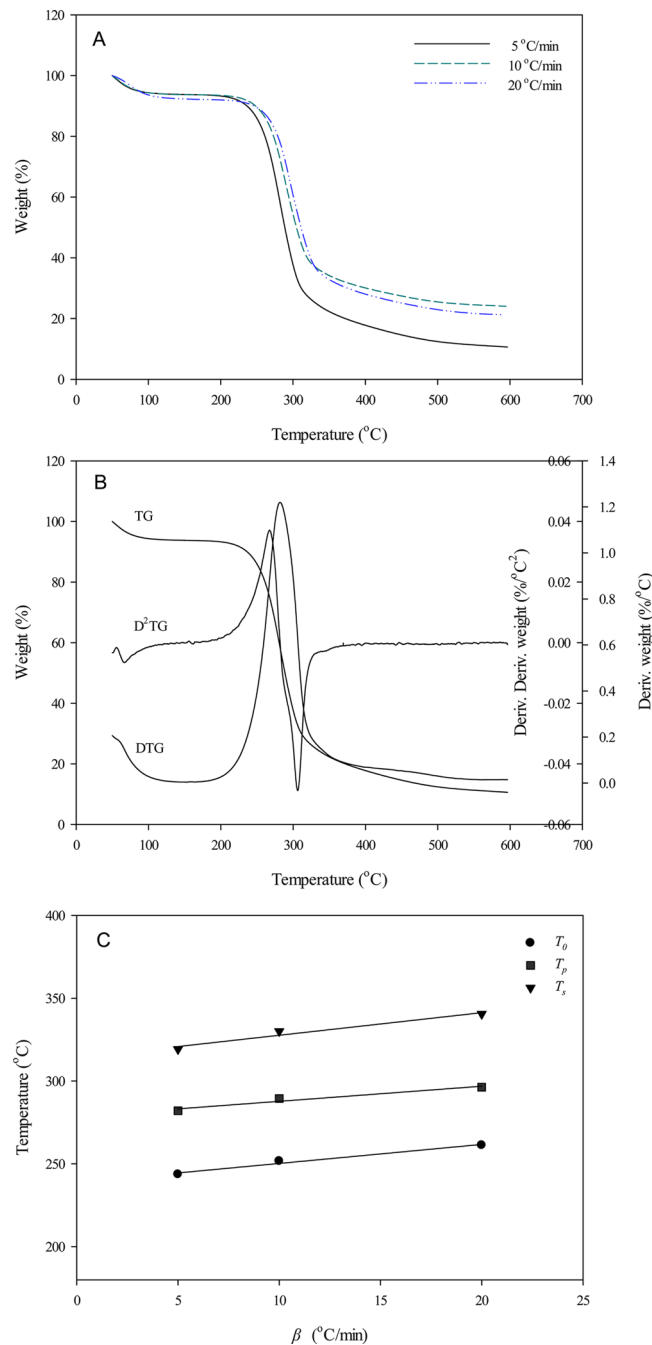


Figure 4. Thermal decomposition analysis of ACAP: (A) TG curves of ACAP at different heating rates; (B) determination of thermal decomposition parameters of ACAP at a heating rate of 5 °C/min; and (C) thermal degradation parameters of ACAP at different heating rates.

Compared with the single-heating rate method, the isoconversional method provides more accurate values of E_a and A .⁴⁰ Therefore, the obtained thermal kinetic parameters had greater practical value to comprehend and predict the thermal degradation process of ACAP. The thermal analysis has been widely performed on cellulose and hemicellulose to obtain the degradation characteristics.^{41,42}

The pyrolysis range of ACAP (238.8–314.0 °C) was found to be consistent with a previous study of several isolated natural polysaccharides, the major weight loss of which occurred in the range of 225–325 °C.⁴¹ In this temperature range (238.8–314.0

Table 3. Degradation Characteristics of ACAP^a

$T_{o\beta\rightarrow 0}$ (°C)	WL _o (%)	$T_{p\beta\rightarrow 0}$ (°C)	WL _p (%)	$T_{s\beta\rightarrow 0}$ (°C)	WL _s (%)	$T_s - T_o$ (°C)	WL _s - WL _o (%)
238.8	2.88	278.6	21.81	314.0	57.24	75.2	54.37

^aData are means. T , temperature; WL, weight loss; subscript o, onset; subscript p, DTG peak; subscript s, shift; subscript $\beta\rightarrow 0$, extrapolated values to the heating rate of 0 °C/min.

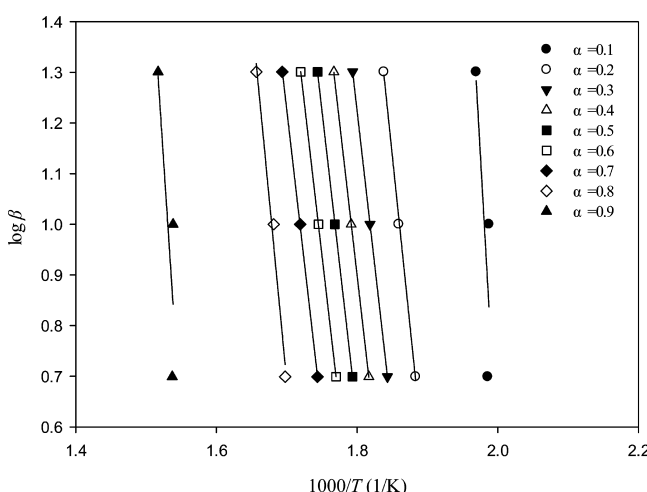


Figure 5. Typical isoconversional plot of Flynn–Wall–Ozawa (FWO) method at different conversion rates.

°C), most of the ACAP (54.37%, Table 3) decomposed to volatiles, including CO, CO₂, CH₄, CH₃COOH, and HCOOH, according to the literature.^{31,43} Moreover, the E_a value of ACAP was determined to be 220.0 kJ/mol, which indicated the good thermal stability of this hemicellulosic heteroxylan. Among these thermal parameters, E_a might indicate a minimum energy requirement to initiate the degradation reaction, with a lower E_a value associated with a lower thermal degradation temperature. These thermal kinetic parameters, including the experimental E_a and A , may also be important for thermal stability evaluation and shelf life prediction of the related polysaccharide products. In other words, the thermal kinetic parameters of ACAP might be important for determining its future applications.

Anti-inflammation Effects of ACAP. ACAP was able to suppress the LPS-induced mRNA expressions of IL-1 β , IL-6, and COX-2 genes in the cultured RAW 264.7 macrophage cells under the experimental conditions (Figure 6). The suppression was dose-dependent for IL-1 β and IL-6 mRNA expressions, but not for COX-2 gene expression. As shown in Figure 6A, 73.98% of IL-1 β mRNA expression was suppressed by ACAP at the final treatment concentration of 50 μ g/mL, whereas the IL-1 β mRNA expression was reduced to 56.80% at 10 μ g/mL. ACAP at 10 μ g/mL reduced the LPS-induced IL-6 mRNA expressions and showed a stronger inhibition effect by 49.38% compared to that at 50 μ g/mL by 31.79% (Figure 6B), suggesting that concentration or dosage may be critical for a desired level of inhibition on IL-6 mRNA expression. Moreover, its inhibitory effects on COX-2 mRNA expression were 20.86 and 26.18% at 50 and 10 μ g/mL final treatment concentrations (Figure 6C), respectively. These results suggested that ACAP might be further developed as a potential functional food ingredient to reduce the risk of inflammation related chronic human diseases.

Hemicelluloses have attracted more and more interest for their environmentally friendly and biosafety properties. Nowadays, hemicellulose has been extensively developed as an important

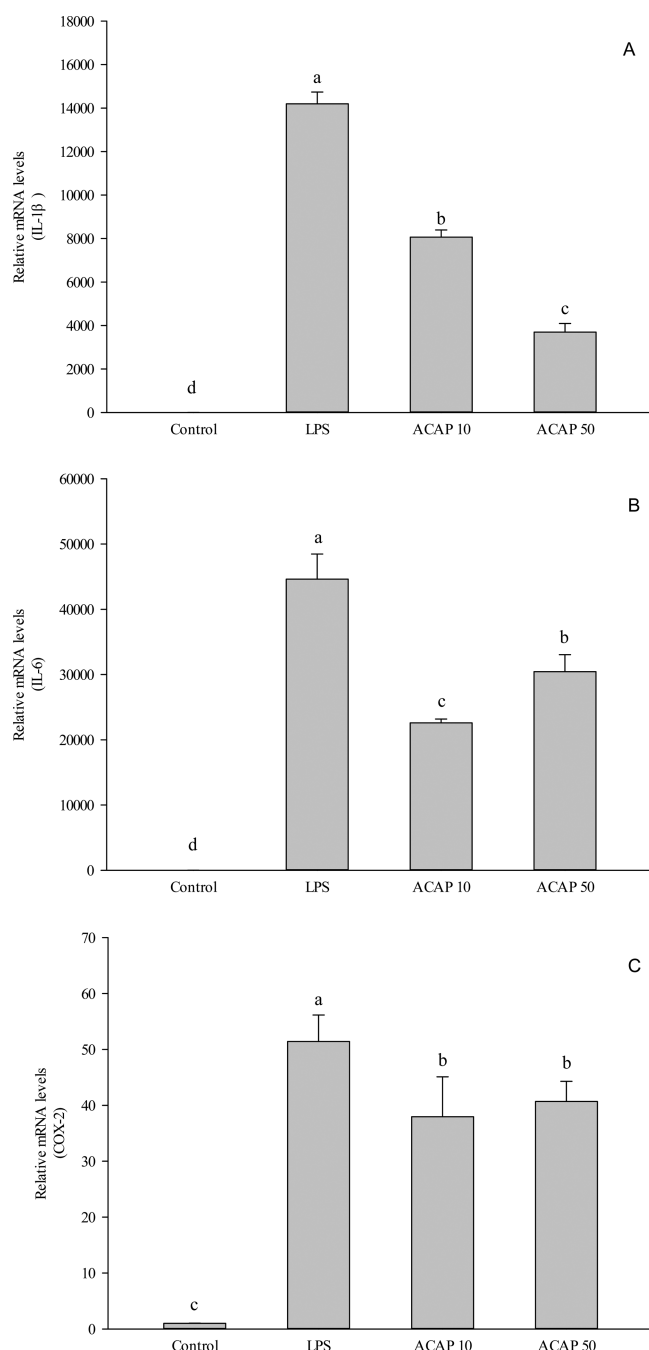


Figure 6. Effects of ACAP on (A) IL-1 β , (B) IL-6, and (C) COX-2 mRNA expressions in LPS-stimulated RAW 264.7 cells. LPS stands for lipopolysaccharide at final concentration of 10 ng/mL; ACAP 10 and ACAP 50 stand for the final treatment concentrations of ACAP at 10 and 50 μ g/mL, respectively. The vertical bars represent the standard deviation ($n = 3$) of each data point. Different letters (a–d) represent significant differences ($P < 0.05$).

biomass in several important fields, including materials, energy, medical, and food industries.^{37,44,45} Alfalfa stem contains

abundant hemicellulosic polysaccharides, but little is known about their chemical structures and functionalities at the molecular level. The structural study of alfalfa polysaccharides remained at the level of the 1960s, which only revealed the monosaccharide composition and partial glycosidic linkages^{3,4} without detailed structural features due to the restriction of prevailing technique and equipment. Elucidation of the structure, pyrolysis features, and anti-inflammatory bioactivity will facilitate the further application of hemicellulosic polysaccharides from alfalfa stem.

In summary, a new hemicellulosic polysaccharide (ACAP) was purified from the cold alkali extract of alfalfa stem and characterized as a heteroxylan, with a molecular weight of 7.94×10^3 kDa and a radius of 58 nm. ACAP contained a β -1→4-linked D-Xylp backbone with 29% short side chains of 4-O-MeGlcA and T-L-Araf units at the O-2 and O-3 branching points, respectively, and had entangled chains. ACAP showed excellent thermal stability with a key decomposition in 238.8–314.0 °C (the extrapolated temperatures) and apparent activation energy E_a and pre-exponential factor A values of 220.0 kJ/mol and 2.81×10^{24} /s, respectively. The thermal characteristic parameters provided a simplified approach to evaluate the thermal decomposition behavior of ACAP in food or industrial applications. In addition, ACAP significantly inhibited the mRNA expressions of the pro-inflammatory cytokine genes, especially for IL-1 β , suggesting its potential anti-inflammatory effect. These results suggested the potential application of ACAP in functional foods and dietary supplement products.

ASSOCIATED CONTENT

Supporting Information

Tables S1 and S2 and Figures S1–S5. This material is available free of charge via the Internet at <http://pubs.acs.org>.

AUTHOR INFORMATION

Corresponding Author

*(L.Y.) Phone: (301) 405-0761. E-mail: lyu5@umd.edu.

Funding

This project was supported by a General Grant from the China Postdoctoral Science Foundation (Grant 2014M561476), a special fund for Agro-scientific Research in the Public Interest (Grant 201203069), a National High Technology Research and Development Program of China (Grants 2013AA102202 and 2013AA102207), SJTU 985-III disciplines platform and talent fund (Grants TS0414115001 and TS0320215001), and a grant from Wilmar (Shanghai) Biotechnology Research & Development Center Co., Ltd.

Notes

The authors declare no competing financial interest.

REFERENCES

- (1) Hu, Y. G.; Cash, D. Global status and development trends of alfalfa. In *Alfalfa Management Guide for Ningxia*; Cash, D., Ed.; Beijing, China, 2009; pp 1–3.
- (2) Lamb, J. F. S.; Jung, H. J. G.; Sheaffer, C. C.; Samac, D. A. Alfalfa leaf protein and stem cell wall polysaccharide yields under hay and biomass management systems. *Crop Sci.* **2007**, *47*, 1407–1415.
- (3) Aspinall, G. O.; McGrath, D. Hemicelluloses of lucerne. *J. Chem. Soc. C* **1966**, 2133–2139.
- (4) Aspinall, G. O.; Fanshawe, R. S. Pectic substances from lucerne (*Medicago sativa*). Part I. Pectic acid. *J. Chem. Soc.* **1961**, 4215–4125.
- (5) Myhre, D. V.; Smith, F. Alfalfa hemicellulose, constitution of the hemicellulose of alfalfa (*Medicago sativa*). Hydrolysis of hemicellulose and identification of neutral and acidic components. *J. Agric. Food Chem.* **1960**, *8*, 359–364.
- (6) Dong, X. F.; Gao, W. W.; Su, J. L.; Tong, J. M.; Zhang, Q. Effects of dietary polysavone (alfalfa extract) and chlortetracycline supplementation on antioxidation and meat quality in broiler chickens. *Br. Poult. Sci.* **2011**, *52*, 302–309.
- (7) Dong, X. F.; Gao, W. W.; Tong, J. M.; Jia, H. Q.; Sa, R. N.; Zhang, Q. Effect of polysavone (alfalfa extract) on abdominal fat deposition and immunity in broiler chickens. *Poult. Sci.* **2007**, *86*, 1955–1959.
- (8) Wang, S. P.; Dong, X. F.; Tong, J. M. Optimization of enzyme-assisted extraction of polysaccharides from alfalfa and its antioxidant activity. *Int. J. Biol. Macromol.* **2013**, *62*, 387–396.
- (9) Liu, H. W.; Dong, X. F.; Tong, J. M.; Zhang, Q. Alfalfa polysaccharides improve the growth performance and antioxidant status of heat-stressed rabbits. *Livest. Sci.* **2010**, *131*, 88–93.
- (10) Deng, W.; Dong, X. F.; Tong, J. M.; Xie, T. H.; Zhang, Q. Effects of an aqueous alfalfa extract on production performance, egg quality and lipid metabolism of laying hens. *J. Anim. Physiol. Anim. Nutr.* **2012**, *96*, 85–94.
- (11) Wang, S. P.; Dong, X. F.; Ma, H.; Cui, Y. M.; Tong, J. M. Purification, characterisation and protective effects of polysaccharides from alfalfa on hepatocytes. *Carbohydr. Polym.* **2014**, *112*, 608–614.
- (12) Hill, M. J. Bacterial fermentation of complex carbohydrate in the human colon. *Eur. J. Cancer Prev.* **1995**, *4*, 353–358.
- (13) Takenaka, S.; Itohama, Y. Rice bran hemicellulose increases the peripheral blood lymphocytes in rats. *Life Sci.* **1993**, *52*, 9–12.
- (14) Ebringerová, A.; Hromádková, Z.; Heinze, T. Hemicellulose. In *Advances in Polymer Science*; Heinze, T., Ed.; Springer: Berlin, Germany, 2005; Vol. 186, pp 1–67.
- (15) Dollinger, G.; Cunico, B.; Kunitani, M.; Johnson, D.; Jones, R. Practical on-line determination of biopolymer molecular weights by high-performance liquid chromatography with classical light-scattering detection. *J. Chromatogr. A* **1992**, *592*, 215–228.
- (16) DuBois, M.; Gilles, K. A.; Hamilton, J. K.; Rebers, P. A.; Smith, F. Colorimetric method for determination of sugars and related substances. *Anal. Chem.* **1956**, *28*, 350–356.
- (17) Blumenkrantz, N.; Asboe-Hansen, G. New method for quantitative determination of uronic acids. *Anal. Biochem.* **1973**, *54*, 484–489.
- (18) Hill, H. D.; Straka, J. G. Protein determination using bicinchoninic acid in the presence of sulfhydryl reagents. *Anal. Biochem.* **1988**, *170*, 203–208.
- (19) Yan, W.; Niu, Y. G.; Lv, J. L.; Xie, Z. H.; Jin, L.; Yao, W. B.; Gao, X. D.; Yu, L. L. Characterization of a heteropolysaccharide isolated from diploid *Gynostemma pentaphyllum* Makino. *Carbohydr. Polym.* **2013**, *92*, 2111–2117.
- (20) Pettolino, F. A.; Walsh, C.; Fincher, G. B.; Bacic, A. Determining the polysaccharide composition of plant cell walls. *Nat. Protoc.* **2012**, *7*, 1590–1607.
- (21) Kim, J. S.; Reuhs, B. L.; Michon, F.; Kaiser, R. E.; Arumugham, R. G. Addition of glycerol for improved methylation linkage analysis of polysaccharides. *Carbohydr. Res.* **2006**, *341*, 1061–1064.
- (22) CCRC. <http://www.ccrc.uga.edu/specdb/ms/pmaa/pframe.html> (accessed Aug 30, 2014).
- (23) Rezanka, T.; Sigler, K. Structural analysis of a polysaccharide from *Chlorella kessleri* by means of gas chromatography-mass spectrometry of its saccharide alditols. *Folia Microbiol. (Praha)* **2007**, *52*, 246–252.
- (24) Chen, L.; Cheung, P. C. K. Mushroom dietary fiber from the fruiting body of *Pleurotus tuber-regium*: fractionation and structural elucidation of nondigestible cell wall components. *J. Agric. Food Chem.* **2014**, *62*, 2891–2899.
- (25) Chen, L.; Zhang, B. B.; Chen, J. L.; Cheung, P. C. K. Cell wall structure of mushroom sclerotium (*Pleurotus tuber-regium*): Part 2. Fine structure of a novel alkali-soluble hyper-branched cell wall polysaccharide. *Food Hydrocolloids* **2014**, *38*, 48–55.
- (26) Flynn, J. H.; Wall, L. A. General treatment of the thermogravimetry of polymers. *J. Res. Natl. Bur. Stand.* **1966**, *70*, 487–523.

- (27) Ozawa, T. A new method of analyzing thermogravimetric data. *Bull. Chem. Soc. Jpn.* **1965**, *38*, 1881–1886.
- (28) Zhang, X. W.; Shang, P. P.; Qin, F.; Zhou, Q.; Gao, B. Y.; Huang, H. Q.; Yang, H. S.; Shi, H. M.; Yu, L. L. L. Chemical composition and antioxidative and anti-inflammatory properties of ten commercial mung bean samples. *LWT—Food Sci. Technol.* **2013**, *54*, 171–178.
- (29) Huang, H. Q.; Cheng, Z. H.; Shi, H. M.; Xin, W. B.; Wang, T. T. Y.; Yu, L. L. L. Isolation and characterization of two flavonoids, engeletin and astilbin, from the leaves of *Engelhardia roxburghiana* and their potential anti-inflammatory properties. *J. Agric. Food Chem.* **2011**, *59*, 4562–4569.
- (30) Hawker, C. J.; Lee, R.; Frechet, J. M. J. One-step synthesis of hyperbranched dendritic polyesters. *J. Am. Chem. Soc.* **1991**, *113*, 4583–4588.
- (31) Sun, S. N.; Cao, X. F.; Xu, F.; Sun, R. C.; Jones, G. L.; Baird, M. Structure and thermal property of alkaline hemicelluloses from steam exploded *Phyllostachys pubescens*. *Carbohydr. Polym.* **2014**, *101*, 1191–1197.
- (32) Kačuráková, M.; Belton, P. S.; Wilson, R. H.; Hirsch, J.; Ebringerová, A. Hydration properties of xylan-type structures: an FTIR study of xylooligosaccharides. *J. Sci. Food Agric.* **1998**, *77*, 38–44.
- (33) Kačuráková, M.; Ebringerová, A.; Hirsch, J.; Hromadkova, Z. Infrared study of arabinoxylans. *J. Sci. Food Agric.* **1994**, *66*, 423–427.
- (34) Jiang, H.; Chen, Q. Q.; Ge, J. H.; Zhang, Y. Efficient extraction and characterization of polymeric hemicelluloses from hybrid poplar. *Carbohydr. Polym.* **2014**, *101*, 1005–1012.
- (35) Kacurakova, M.; Capek, P.; Sasinkova, V.; Wellner, N.; Ebringerova, A. FT-IR study of plant cell wall model compounds: pectic polysaccharides and hemicelluloses. *Carbohydr. Polym.* **2000**, *43*, 195–203.
- (36) Ebringerova, A.; Hromadkova, Z.; Alföldi, J.; Berth, G. Structural and solution properties of corn cob heteroxylans. *Carbohydr. Polym.* **1992**, *19*, 99–105.
- (37) Capek, P.; Matulová, M. An arabino(glucurono)xyan isolated from immunomodulatory active hemicellulose fraction of *Salvia officinalis* L. *Int. J. Biol. Macromol.* **2013**, *59*, 396–401.
- (38) Sun, S. L.; Wen, J. L.; Ma, M. G.; Sun, R. C. Successive alkali extraction and structural characterization of hemicelluloses from sweet sorghum stem. *Carbohydr. Polym.* **2013**, *92*, 2224–2231.
- (39) Peng, Y. Y.; Wu, S. B. The structural and thermal characteristics of wheat straw hemicellulose. *J. Anal. Appl. Pyrol.* **2010**, *88*, 134–139.
- (40) Vyazovkin, S. Model-free kinetics. Staying free of multiplying entities without necessity. *J. Therm. Anal. Calorim.* **2006**, *83*, 45–51.
- (41) Iqbal, M. S.; Massey, S.; Akbar, J.; Ashraf, C. M.; Masih, R. Thermal analysis of some natural polysaccharide materials by isoconversional method. *Food Chem.* **2013**, *140*, 178–182.
- (42) Yao, F.; Wu, Q. L.; Lei, Y.; Guo, W. H.; Xu, Y. J. Thermal decomposition kinetics of natural fibers: activation energy with dynamic thermogravimetric analysis. *Polym. Degrad. Stab.* **2008**, *93*, 90–98.
- (43) Maschio, G.; Koufopanos, C.; Lucchesi, A. Pyrolysis, a promising route for biomass utilization. *Bioresour. Technol.* **1992**, *42*, 219–231.
- (44) Ragauskas, A. J.; Williams, C. K.; Davison, B. H.; Britovsek, G.; Cairney, J.; Eckert, C. A.; Frederick, W. J.; Hallett, J. P.; Leak, D. J.; Liotta, C. L. The path forward for biofuels and biomaterials. *Science* **2006**, *311*, 484–489.
- (45) Pan, X. J.; Arato, C.; Gilkes, N.; Gregg, D.; Mabee, W.; Pye, K.; Xiao, Z. Z.; Zhang, X.; Saddler, J. Biorefining of softwoods using ethanol organosolv pulping: preliminary evaluation of process streams for manufacture of fuel-grade ethanol and co-products. *Biotechnol. Bioeng.* **2005**, *90*, 473–481.